Calibration-free wavelength modulation spectroscopy for gas concentration measurements under low-absorbance conditions*

Che Lu(车 璐), Ding Yan-Jun(丁艳军)†, Peng Zhi-Min(彭志敏), and Li Xiao-Hang(李晓航)

State Key Laboratory of Power Systems, Department of Thermal Engineering, Tsinghua University, Beijing 100084, *China*

(Received 18 April 2012; revised manuscript received 6 May 2012)

We derive the expressions of the first and second harmonic signals on the basis of absorption spectral and lock-in theories, and determine the gas concentration according to the ratio of second and first harmonic signals. It is found that the X and Y components of the harmonic signals are influenced by the phase shift between the detection and reference signal, and the phase shift can be any value in a range from 0 to 2π, which is different from the results obtained previously. Meanwhile, an additional item caused by the residual amplitude modulation will make a great contribution to the second harmonic signal, and may not be neglected under low absorbance conditions. Theoretical analysis indicates that subtracting back-ground signal from the second harmonic signal can remove the influence of this item, and can improve the measurement accuracy of gas concentration. On this basis, we select the transition of CO_2 at 6527.64 cm^{-1} to analyse the approximation errors during the derivation by numerical simulation and then measure the CO_2 concentration under low absorbance conditions, with absorbance varying from 1‰ to 6‰.

Keywords: tunable diode laser absorption spectroscopy, wavelength modulation spectroscopy, harmonic signals, low absorbance conditions

PACS: 78.40.–q, 78.30.–j, 42.68.Ca **DOI:** 10.1088/1674-1056/21/12/127803

1. Introduction

With the development of the tunable diode laser absorption spectroscopy (TDLAS) and the improvement of the accuracy for measuring gas concentration, the direct absorption spectroscopy, easily affected by particle concentration, laser intensity fluctuation, transition overlapping, and baseline fitting error that often hampers the accurate determination of line shape, has become more and more difficult to meet the measurement requirements.[1−3] Wavelength modulation spectroscopy (WMS) has a high sensitivity to gas concentration measurements under low absorbance conditions,[4−6] while it cannot determine gas concentration directly from the harmonic signals without calibration experiments in the early stage.[7,8] Recently, a calibration-free method based on residual amplitude modulation (RAM) was developed in Refs. [9]–[11], where the first harmonic (1f) signal is used to normalize the second harmonic (2f) signal, therefore, removing the effects of laser intensity fluctuation and electro–optical gain, and an expression which can be used to determine gas concentration is derived when the absorbance is less than 5.0%.[12]

However, in these studies, the phase shift between the detection and reference signals during the derivation of the 1f and 2f signals was neglected, and the phase shift was approximated to zero. While in practical measurements, the phase shift is influenced by the measurement system and varies with the frequency of the reference signal, and can be any value in a range from 0 to 2π. Meanwhile, in order to obtain the gas concentration expression, the 1f and 2f signals were simplified during the derivation, especially the additional item in the 2f signal caused by RAM was neglected in some cases, and these approximation errors were not analysed in previous studies.

In this paper, we derive the expressions of the 1f and 2f signals according to the absorption spectral and lock-in theories. The influence caused by the phase shift between the detection and reference signal on the harmonic signal is analyzed, and the gas concentration may be determined directly from the ratio of the 2f signal (the additional item has been

*Project supported by the National Natural Science Foundation of China (Grant Nos. 51176085 and 51206086).

†Corresponding author. E-mail: dyj@mail.tsinghua.edu.cn

© 2012 Chinese Physical Society and IOP Publishing Ltd

removed) and the 1f signal (2f/1f).[13] Then, the transition of CO_2 at 6527.64 cm^{-1} is selected to analyse the measurement errors caused by the approximation during the derivation both in simulation and practical measurement under low absorbance conditions.

2. Measurement principles

The laser transmission of monochromatic radiation at frequency ν through a uniform medium is described by the Beer–Lambert law, and when the absorbance is less than 5.0%, the Beer–Lambert law can be expanded by a first-order Taylor series as follows:

$$\tau(v) = \frac{I_t}{I_0} = \exp[-PS(T)Lx\varphi(v)] \approx 1 - \xi x\varphi(v) = 1 - \xi x \cdot \sum_{k=0}^{\infty} H_k \cdot \cos(k\omega t), \quad (1)$$

where $\tau(\nu)$ is the transmission coefficient; I_0 and I_t are the incident and transmitted laser intensity, respectively; P in atm is the total gas pressure; $S(T)$ in $cm^{-2}\cdot atm^{-1}$ (1 atm = 1.01325×10^5 Pa) is the line strength; x is the mole fraction of the absorbing species; L in cm is the absorption path length; $\varphi(\nu)$ in cm is the line-shape function expressed by the Voigt profile,[14] $\xi = PS(T)L$; ω is the modulation frequency; H_k is given as

$$\begin{cases} H_0 = \dfrac{1}{2\pi}\int_{-\pi}^{\pi}\varphi(v)\,\mathrm{d}\theta, \\ H_k = \dfrac{1}{\pi}\int_{-\pi}^{\pi}\varphi(v)\cos k\theta\,\mathrm{d}\theta, \ k = 1, 2, 3, \ldots \end{cases} \quad (2)$$

The incident laser intensity is also simultaneously modulated and given by[9]

$$I_0 = I + \Delta I_1 \cos(\omega t + \psi_1) + \Delta I_2 \cos(2\omega t + \psi_2), \quad (3)$$

where I is the average laser intensity; ΔI_1 and ΔI_2 are the amplitudes of linear and the first nonlinear laser intensity modulation, respectively; ψ_1 and ψ_2 are the phase shifts between intensity modulation and wavelength modulation for linear and nonlinear intensity modulation, respectively.

Substituting Eq. (3) into Eq. (1), the expressions of first and second components of the transmitted intensity I_t can be written as

$$\begin{cases} V_{sig-1} = F_{11}\cos\omega t + F_{12}\sin\omega t, \\ V_{sig-2} = F_{21}\cos 2\omega t + F_{22}\sin 2\omega t, \end{cases} \quad (4)$$

where F_{11}, F_{12}, F_{21}, and F_{22} are given as

$$\begin{cases} F_{11} = -\xi x I H_1 + \Delta I_1\Big[1 - \xi x\Big(H_0 + \dfrac{H_2}{2}\Big)\Big]\cos\psi_1 - \xi x\dfrac{\Delta I_2}{2}(H_1 + H_3)\cos\psi_2, \\ F_{12} = \Delta I_1\Big[\xi x\Big(H_0 - \dfrac{H_2}{2}\Big) - 1\Big]\sin\psi_1 + \xi x\dfrac{\Delta I_2}{2}(H_1 - H_3)\sin\psi_2, \\ F_{21} = -\xi x I H_2 - \xi x\dfrac{\Delta I_1}{2}(H_1 + H_3)\cos\psi_1 + \Delta I_2\Big[1 - \xi x\Big(H_0 + \dfrac{H_4}{2}\Big)\Big]\cos\psi_2, \\ F_{22} = \xi x\dfrac{\Delta I_1}{2}(H_1 - H_3)\sin\psi_1 + \Delta I_2\Big[\xi x\Big(H_0 - \dfrac{H_4}{2}\Big) - 1\Big]\sin\psi_2. \end{cases} \quad (5)$$

The lock-in amplifier amplifies the transmitted intensity and multiplies the signal by the reference signal using a phase-sensitive detector (PSD). Then the harmonic signal passes through a low pass filter, and the AC signals are removed, while the DC signals remain there. The X and Y components of the reference signal are given as

$$\begin{cases} X : V_{ref-k} = R\cos(k\omega t + \theta_k), \\ Y : V_{ref-k} = R\sin(k\omega t + \theta_k), \end{cases} \quad (6)$$

where R is the amplitude of the reference signal, θ_k is the phase shift between the detection signal and the k-th reference signal. The X and Y components of 1f and 2f signals from the lock-in amplifier can be written as follows:

$$\begin{cases} X_{1f} = \dfrac{GR}{2}(F_{11}\cos\theta_1 - F_{12}\sin\theta_1), \\ Y_{1f} = \dfrac{GR}{2}(F_{11}\sin\theta_1 + F_{12}\cos\theta_1), \\ X_{2f} = \dfrac{GR}{2}(F_{21}\cos\theta_2 - F_{22}\sin\theta_2), \\ Y_{2f} = \dfrac{GR}{2}(F_{21}\sin\theta_2 + F_{22}\cos\theta_2), \end{cases} \quad (7)$$

where G is the electro–optical gain of the system.

In Eq. (7), the X and Y components of the 1f and 2f signals are influenced by the phase shifts (θ_1, θ_2) between the detection and reference signals. Each of the phase shifts is determined by the measurement system and varies with the frequency of the reference signal, and can be any value in a range from 0 to 2π. Therefore, the phase shifts should be measured accurately in practical measurements. For example,

the phase shift θ_2 in Fig. 4 is about $-130°$ in the experiment. However in the previous studies the effects of these phase shifts were ignored and assumed to be zero. Perhaps, the phase shifts can be adjusted to be zero by regulating the phase of the reference signal according to the experimental results (when the Y component of the 2f signal is zero) under high absorbance conditions. However, under low absorbance conditions discussed in this paper, the RAM gives rise to an additional item in the 2f signal (evidently seen in Eq. (10)) which may not be ignored, the phase shifts can hardly be adjusted to be zero in practical experiments. When the phase shifts are assumed to be zero, the X and Y components of 1f and 2f signals are simplified into the following case,[7] which is a special case in practical measurements:

$$\begin{cases} X_{1\mathrm{f}} = \dfrac{GR}{2}F_{11}, & Y_{1\mathrm{f}} = \dfrac{GR}{2}F_{12}, \\ X_{2\mathrm{f}} = \dfrac{GR}{2}F_{21}, & Y_{2\mathrm{f}} = \dfrac{GR}{2}F_{22}. \end{cases} \tag{8}$$

In actual measurements, the amplitudes of the 1f and 2f signals at the line centre are used to determine the gas temperature or gas concentration. As is well known, at the line centre, $H_1 = H_3 = 0$, and when the absorbance is very low (say, less than 5.0%), $\xi x H_0$, $\xi x H_2$, $\xi x H_4 \ll 1$, the X and Y components of the 1f and 2f signals can be simplified into the following case where $S_{1\mathrm{f}}$ and $S_{2\mathrm{f}}$ represent the amplitudes of the 1f and 2f signals at the line centre, respectively (their approximation errors during the derivation are analyzed in Section 4):

$$\begin{cases} X_{1\mathrm{f}} \approx \dfrac{GR}{2}\Delta I_1 \cos(\psi_1 - \theta_1) \\ Y_{1\mathrm{f}} \approx \dfrac{GR}{2}\Delta I_1 \sin(\psi_1 - \theta_1) \end{cases} \Rightarrow S_{1\mathrm{f}} = \sqrt{X_{1\mathrm{f}}^2 + Y_{1\mathrm{f}}^2} \approx \frac{GR}{2}\Delta I_1, \tag{9}$$

$$\begin{cases} X_{2\mathrm{f}} \approx -\dfrac{GR}{2}\xi x I H_2 \cos\theta_2 + \dfrac{GR\Delta I_2}{2}\cos(\psi_2 - \theta_2) \\ Y_{2\mathrm{f}} \approx -\dfrac{GR}{2}\xi x I H_2 \sin\theta_2 + \dfrac{GR\Delta I_2}{2}\sin(\psi_2 - \theta_2) \end{cases} \Rightarrow S_{2\mathrm{f}} = \sqrt{X_{2\mathrm{f}}^2 + Y_{2\mathrm{f}}^2}. \tag{10}$$

In Eq. (10), the amplitude of the 2f signal has an additional item caused by RAM (the amplitude of the nonlinear laser modulation ΔI_2). Simulation and experiment results indicate that the additional item has the same magnitudes or even larger than the previous item (which contains the gas temperature and concentration information) under low absorbance conditions, and there is no linear correlation between the 2f amplitude and gas concentration. So the influence of the additional item should be removed from the 2f signal in practical measurements.

During our derivation, we have found that when there is no absorption ($x = 0$), which is called the back-ground signal, the X and Y components of the 2f signal of the back-ground signal at the line centre can be written as

$$\begin{cases} X_{2\mathrm{f-back}} = \dfrac{GR\Delta I_2}{2}\cos(\psi_2 - \theta_2), \\ Y_{2\mathrm{f-back}} = \dfrac{GR\Delta I_2}{2}\sin(\psi_2 - \theta_2). \end{cases} \tag{11}$$

Comparing Eq. (10) with Eq. (11), subtracting the back-ground signal from the X and Y components of the original 2f signal in Eq. (10), the amplitude of the subtracted 2f signal can be written as

$$\begin{aligned} S'_{2\mathrm{f}} &= \sqrt{(X_{2\mathrm{f}} - X_{2\mathrm{f-back}})^2 + (Y_{2\mathrm{f}} - Y_{2\mathrm{f-back}})^2} \\ &\approx \frac{GR}{2}\xi x I H_2. \end{aligned} \tag{12}$$

As shown in Eq. (12), the additional item caused by RAM has been removed from the subtracted 2f signal. Normalizing the subtracted 2f signal by the 1f signal, the gas concentration can be determined by the following WMS 2f/1f method:

$$\begin{aligned} S = \frac{S'_{2\mathrm{f}}}{S_{1\mathrm{f}}} &\approx -\frac{\xi x H_2}{\Delta I_1 / I} = -\frac{PS(T)LxH_2}{\Delta I_1 / I} \\ \Rightarrow x &= -\frac{S \cdot \Delta I_1 / I}{PS(T)LH_2}. \end{aligned} \tag{13}$$

3. Experiments setup

Figure 1 illustrates the experimental setup used to determine the CO_2 concentration under low-absorbance conditions (absorbance varies from 1‰ to 6‰). The distributed feedback diode laser (1531 nm, 10 mW, NLK1S5AAA) is used as the spectroscopic source. The laser current and temperature are controlled using a commercial diode laser controller (ITC4001). The fiber-coupled laser passes through a fiber collimator (F280 APC-1550) and is then sent through a 120-cm long gas cell filled with CO_2/N_2 mixture. The transmitted laser intensity is detected

using a large-surface Ge photodiode (PDA 50B-EC), and the detected signal is divided into two beams: one is recorded using a digital oscilloscope (DPO 7014B) and the other is sent into the lock-in amplifier (SR830) to acquire the harmonic signals. Both the modulation and the reference signals are generated from the lock-in amplifier in Fig. 1. Prior to each experiment, the gas cell is evacuated using a vacuum pump to an ultimate pressure of 1.0 Pa and filled with CO_2/N_2 mixture controlled by two mass flow controllers ($0 \sim 10$ mL/min for CO_2 and $0 \sim 10$ L/min for N_2, respectively) according to the experimental requirements. Then, the gas temperature and pressure can be measured accurately in the experiment.

In the present paper, the transition of CO_2 at 6527.64 cm^{-1} was selected for the laser parameter calibration and the CO_2 concentration measurement. The spectroscopic parameters of the transition are acquired from HITRAN 2008 database and are shown in Table 1.

Table 1. Spectroscopic parameters for the selected CO_2 transition (296 K).

v_0/cm^{-1}	E/cm^{-1}	$S/(cm^{-2}/atm)$	$\gamma_{self}/(cm^{-1}/atm)$	$\gamma_{air}/(cm^{-1}/atm)$
6527.64	464.17	1.65×10^{-5}	0.0880	0.0687

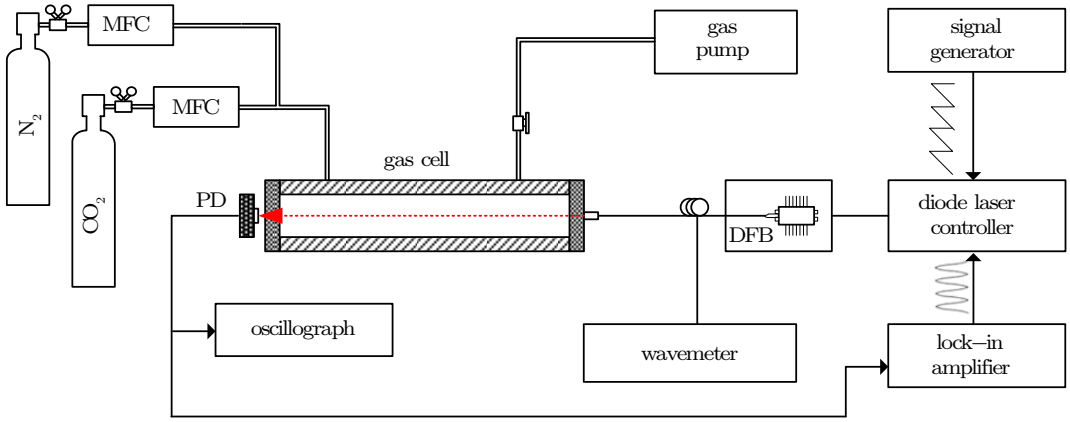


Fig. 1. Experimental setup for measuring CO_2 concentration.

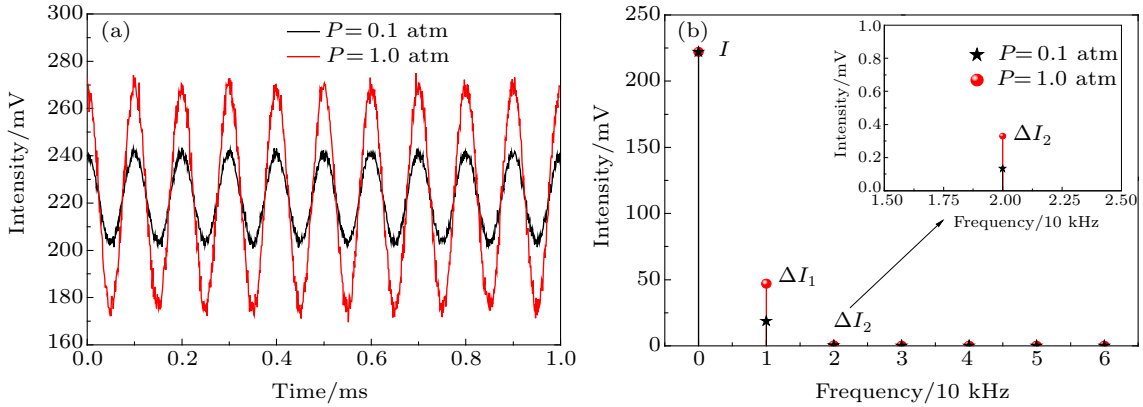


Fig. 2. (colour online) (a) Detected original signals and (b) fast Fourier transform components of the original signals.

As noted in Eq. (13), the laser parameters (ΔI_1, I) need to be calibrated prior to practical experiments using the original laser signal. During the calibration, the laser wavelength was tuned absolutely to the line centre and then modulated with a 10-kHz sinusoidal waveform, where the modulation depth varies with the half width at half maximum (HWHM), which was determined by gas temperature, concentration, and pressure of the selected transition. Figure 2 shows two typical calibration results, the original signals (Fig. 2(a)), and their fast Fourier transform (FFT) components (Fig. 2(b)). As shown in Fig. 2(b), at the line centre, $I = 222.15$ mV, $\Delta I_1 = 18.75$ mV, $\Delta I_2 = 0.1332$ mV when the total pressure is 0.1 atm, and

$I = 222.15$ mV, $\Delta I_1 = 46.85$ mV, $\Delta I_2 = 0.3281$ mV when the total pressure is 1.0 atm.

4. Analysis of the approximation errors

According to the derivation in Section 2, under low absorbance conditions, $\xi x H_0$, $\xi x H_2$, $\xi x H_4 \ll 1$, we have approximated them to zero to derive the 1f and subtracted 2f amplitudes at the line centre as shown in Eqs. (9) and (12), while in actual measurements, these parameters mentioned above are not exactly equal to zero. So the approximation will result in approximation errors in 1f and subtracted 2f amplitudes. In this section, we analyse the approximation errors with numerical simulations on the basis of parameters calibrated above and set the simulation conditions to be similar to those for the practical measurements, where the laser parameters are as follows: $\Delta I_1/I \in [0.1, 0.3]$, $\Delta I_2/I \in [7 \times 10^{-4}, 2.1 \times 10^{-3}]$, $\psi_1 \in [0, \pi]$, $\psi_2 \in [0, \pi]$. The gas temperature, total pressure, and absorption path length are 296 K, 1.0 atm, and 120 cm, respectively. Meanwhile, the CO_2 concentration varies from 20% to 80%, and the absorbance at the line centre varies from 1‰ to 6‰ The simulation results are shown in Figs. 3 and 4.

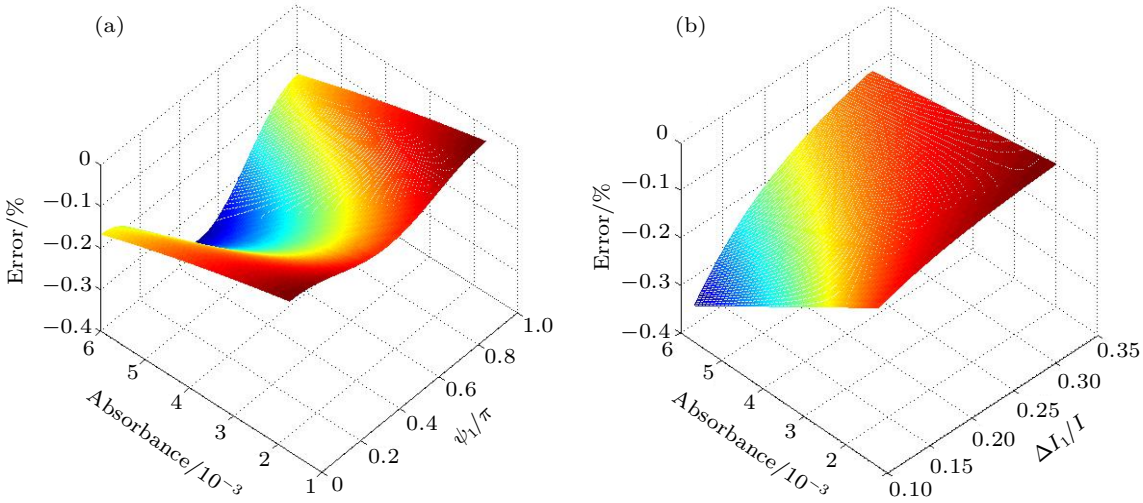


Fig. 3. (colour online) (a) Approximation errors of 1f amplitude with absorbance and phase shift of linear modulation (assuming $\Delta I_1/I = 0.21$) and (b) approximation errors of 1f amplitude with absorbance and the amplitude of linear modulation (assuming $\psi_1 = \pi$).

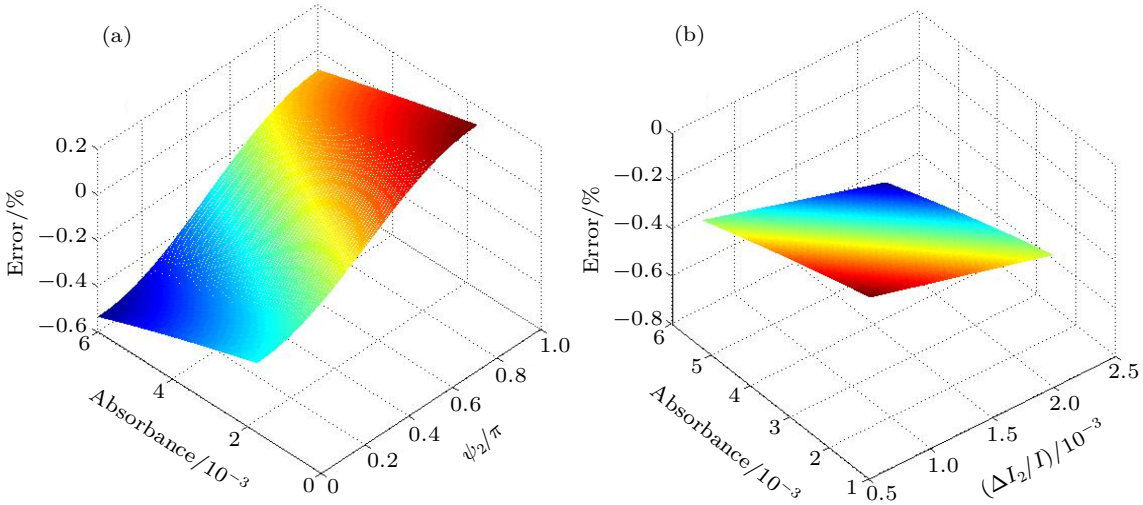


Fig. 4. (colour online) (a) Approximation errors of subtracted 2f amplitude with the absorbance and phase shift of nonlinear modulation (assuming $\Delta I_2/I = 1.47 \times 10^{-3}$) and (b) approximation errors of subtracted 2f amplitude with the absorbance and amplitude of nonlinear modulation (assuming $\psi_2 = \pi$).

The approximation errors of 1f amplitude are shown in Fig. 3, where the approximation errors vary with the absorbance, phase shift (ψ_1) and amplitude of the linear modulation (ΔI_1). The simulation results show that the approximation errors decrease as the absorbance decreases, and the maximum approximation error of the 1f amplitude is no more than -0.4% when the absorbance is less than 6‰ so the approximation errors of 1f amplitude can be ignored under such low absorbance conditions.

Similar to Fig. 3, figure 4 shows the approximation errors of the subtracted 2f amplitude as shown in Eq. (12), where the background signal is subtracted from the origin 2f signal. In Fig. 4, the approximation errors vary with the absorbance, phase shift (ψ_2), and amplitude of the nonlinear modulation (ΔI_2) and are no more than -0.6%, which can be neglected in gas concentration measurements under such low absorbance conditions. The simulation results also indicate that subtracting the background signal from the original 2f signal can efficiently remove the influence of the additional item caused by RAM.

5. Experimental results

A typical experimental result is shown in Fig. 5 in order to illustrate the influence on the 2f signal caused by RAM. In the experiment, the laser wavelength is tuned using a saw-tooth waveform of 40 Hz from the signal generator together with a high frequency sinusoidal waveform of 10 kHz from the lock-in amplifier and the modulation depth is ± 0.063 cm^{-1}. The gas temperature, total pressure, CO_2 concentration, and absorption path length are 296 K, 0.1 atm, 70.05% and 120 cm, respectively, other parameters are measured and they are $I = 222.15$ mV, $\Delta I_1 = 18.75$ mV, the absorbance and 1f amplitude at the line centre: 4.26‰ and 3.25 V, respectively.

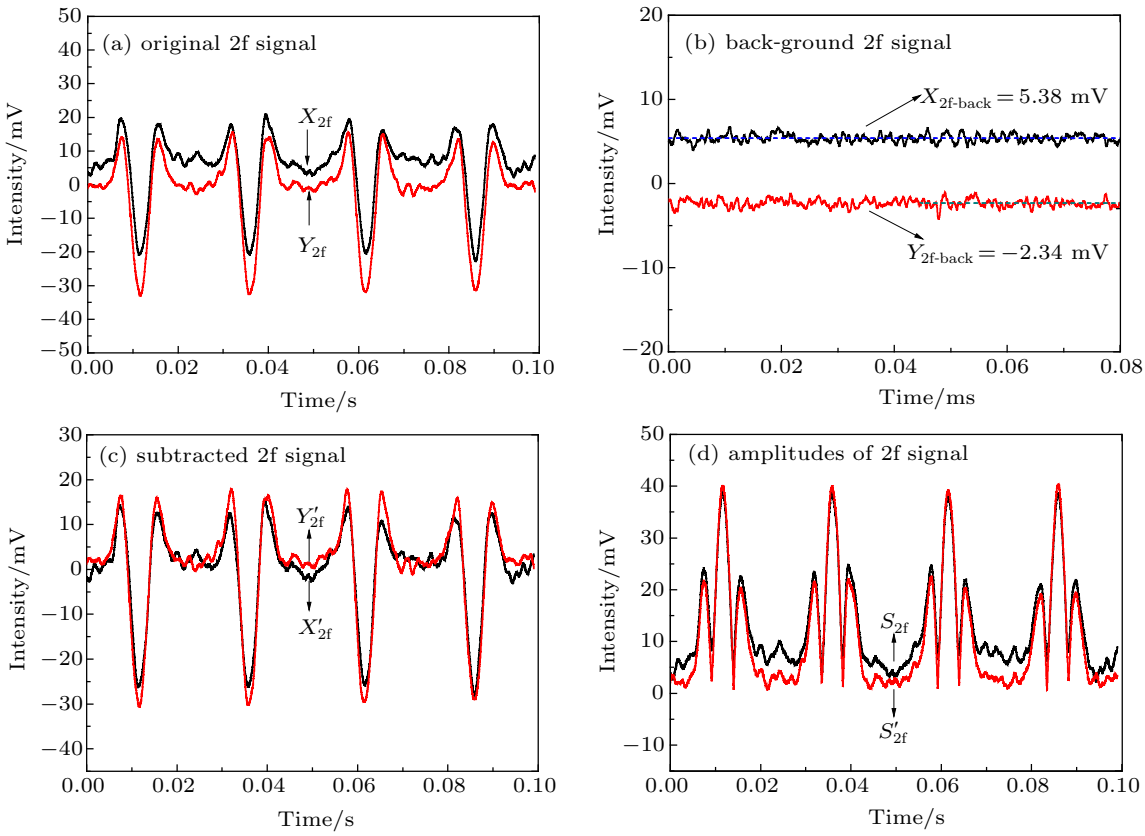


Fig. 5. (colour online) (a) The X and Y components of the original 2f signal; (b) X and Y components of the background 2f signal; (c) X and Y components of the subtracted 2f signal; (d) amplitudes of the original and subtracted 2f signals.

Figure 5(a) shows the X and Y components of the original 2f signal, and figure 5(b) shows the X and Y components of the background 2f signal. Subtracting the background signal from the original 2f signal, the obtained X and Y components of the subtracted 2f signal are shown in Fig. 5(c). The lines in Fig. 5(d) represent the amplitudes of the original 2f signal (S_{2f}) and subtracted 2f signal (S'_{2f}), and the values of S_{2f}

and S'_{2f} at the line centres are about 39.28 mV and 40.68 mV, respectively. Substitute S_{2f} and S'_{2f} into Eq. (13), then the CO_2 concentrations will be calculated to be 67.75% (using S_{2f}) and 70.17% (using S'_{2f}), with measurement errors being −3.28% and 0.17%, respectively.

In practical measurements, we only need to acquire the amplitudes of the 1f and 2f signals at the line center. So we can tune the laser wavelength exactly to the line centre (6527.64 cm^{-1}) using a wavelength meter, then modulate the wavelength with a 10-kHz sinusoidal waveform from the lock-in amplifier, and the modulation depth is ±0.168 cm^{-1}. Figure 6 shows a typical experimental result, where the gas temperature, total pressure, CO_2 concentration, and absorption path length are 296 K, 1 atm, 70.05%, and 120 cm, respectively, other parameters are measured and they are $I = 222.15$ mV, $\Delta I_1 = 46.85$ mV, the absorbance and 1f amplitude at the line centre: 5.34‰ and 3.1003 V, respectively.

Figure 6 (a) shows the X and Y components of original and background 2f signals at the line centres, from the lock-in amplifier. The amplitudes of the original and subtracted 2f signals at the line centres are shown in Fig. 6(b), where the values of S_{2f} and S'_{2f} are 28.605 mV and 26.681 mV, respectively. Substitute S_{2f} and S'_{2f} into Eq. (13), then the CO_2 concentration will be calculated to be 74.58% (using S_{2f}) and 69.57% (using S'_{2f}), with measurement errors being 6.47% and −0.69%, respectively.

In a way similar to that for Fig. 6, in the following experiments, we fix the parameters of the DFB laser, and measure the CO_2 concentrations in different CO_2/N_2 mixtures. The CO_2 concentration varies from 20% to 80%, and the absorbance at the line centre varies from 1‰ to 6‰. The measured CO_2 concentrations are shown in Table 2, where the CO_2 concentrations calculated from the subtracted 2f signals are in good agreement with their corresponding true values, with a measuring error being no more than 2.0% when the absorbance varies from 1‰ to 6‰. While the concentrations of CO_2 obtained from the original 2f signals (where the background 2f signal is not removed) have large measurement errors under low absorbance conditions, especially when the CO_2 concentration is 20% (absorbance is 1.68‰), the measurement error goes up to 310%, leading to erroneous measurement results. The measurement results indicate that under low absorbance conditions, subtracting the 2f signal of the background signal from the original 2f signal can remove the influence of the additional item caused by RAM, and then leads to a good measurement accuracy for the WMS 2f/1f method.

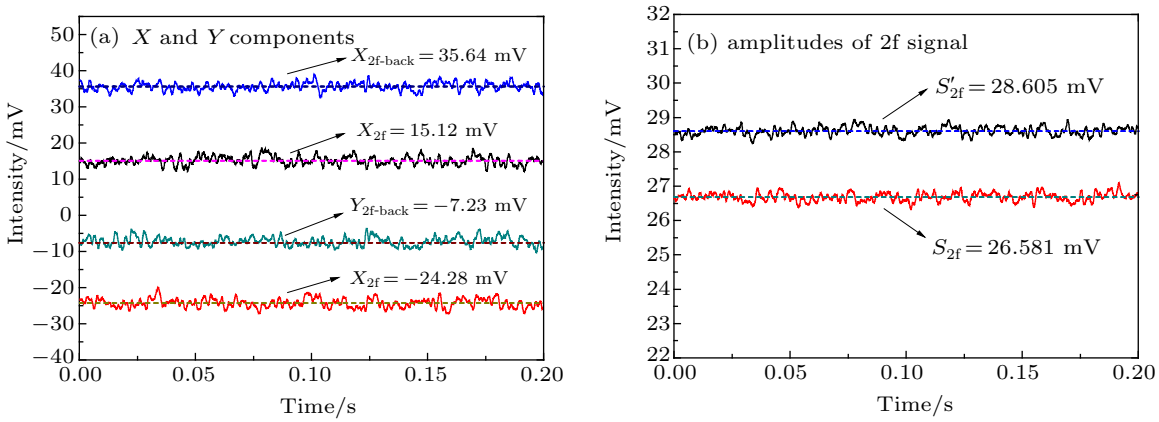


Fig. 6. (colour online) (a) The X and Y components of the original and background 2f signals in the line centre and (b) amplitudes of the original and subtracted 2f signals at the line centre.

Table 2. Measurement results of CO_2 concentration.

True concentration of CO_2/%	Absorbance at the line center/%	Measured results based on subtracted 2f signals		Measured results based on original 2f signals	
		Concentration/%	Error/%	Concentration/%	Error/%
80.06	5.97	79.02	−1.29	77.29	3.47
70.05	5.34	69.57	−0.69	74.58	6.47
60.38	4.71	59.24	−1.89	72.40	19.90
49.90	3.99	49.01	−1.78	82.91	66.14
40.24	3.30	40.83	1.48	82.17	104.20
29.92	2.52	30.42	1.67	78.21	161.41
19.44	1.68	19.35	−0.45	79.57	309.32

6. Conclusions

The X and Y components of the 1f and 2f signals are derived according to the absorption spectral and lock-in theories in this paper, where the phase shift between the detection and the reference signal, influenced by the measurement system and the frequency of the reference signal, can be any value in a range from 0 to 2π, and the expressions indicate that the X and Y components of the harmonic signals vary with phase shift. Then the X and Y components are simplified and the expression of the gas concentration based on the ratio between the 2f and 1f signals is derived. It is theoretically proved that subtracting the background signal from the original 2f signal can efficiently remove the influence of the additional item caused by RAM. The approximation errors during the derivation are analysed in numerical simulation and then the transition of CO_2 at 6527.64 cm^{-1} is selected to measure the CO_2 concentration using the calibration-free WMS 2f/1f method under low absorbance conditions (with absorbance varying from 1‰ to 6‰). The results indicate that the WMS 2f/1f method keeps a good accuracy under low absorbance conditions, which will be widely used in gas concentration measurements in the future.

References

[1] Wagner S, Fisher B T, Fleming J W and Ebert V 2009 *Proc. Combust. Ins.* **32** 839

[2] Farooq A, Jeffries J B and Hanson R K 2008 *Appl. Phys.* B **90** 619

[3] Liu J T C, Jeffries J B and Hanson R K 2004 *Appl. Phys.* B **78** 503

[4] Reid J and Labrie D 1981 *Appl. Phys.* B **26** 203

[5] Cai T D, Jia H, Wang G S, Chen W D and Gao X M 2009 *Sens. Actuators* A **152** 5

[6] Che L, Ding Y J, Peng Z M and Li X H 2012 *Chin. Phys. Lett.* **29** 067801

[7] Rieker G B, Jeffries J B and Hanson R K 2009 *Appl. Opt.* **48** 5546

[8] Wang F, Cen K F, Li N, Huang Q X, Chao X, Yan J H and Chi Y 2010 *Flow Meas. Instrum.* **21** 382

[9] Li H, Rieker G B, Liu X, Jeffries J B and Hanson R K 2006 *Appl. Opt.* **45** 1052

[10] Farooq A, Jeffries J B and Hanson R K 2009 *Appl. Phys.* B **96** 161

[11] Rieker G B, Jeffries J B, Hanson R K, Mathur T, Gruber M R and Carter C D 2009 *Proc. Combust. Inst.* **32** 831

[12] Peng Z M, Ding Y J, Che L, Ling X H and Zheng K J 2011 *Opt. Express* **19** 23104

[13] Kluczynski P and Axner O 1999 *Appl. Opt.* **38** 5803

[14] Tommasi E D, Castrillo A, Casa G and Gianfrani L 2008 *J. Quantum Spectrosc. Radiat. Transf.* **109** 168